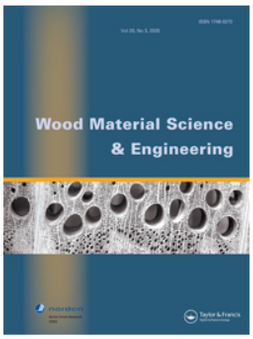

Wood Material Science & Engineering

ISSN: 1748-0272 (Print) 1748-0280 (Online) Journal homepage: www.tandfonline.com/journals/swoo20

Vacuum infiltration of biobased and synthetic polymers for enhancing wood properties in construction

Maria Naissi, Andrija Pranjic, Steliyana Yancheva & Martin Trautz

To cite this article: Maria Naissi, Andrija Pranjic, Steliyana Yancheva & Martin Trautz (08 Jul 2025): Vacuum infiltration of biobased and synthetic polymers for enhancing wood properties in construction, Wood Material Science & Engineering, DOI: 10.1080/17480272.2025.2521632

To link to this article: https://doi.org/10.1080/17480272.2025.2521632

Published online: 08 Jul 2025.

WOOD MATERIAL SCIENCE & ENGINEERING
https://doi.org/10.1080/17480272.2025.2521632

Taylor & Francis
Taylor & Francis Group

ORIGINAL ARTICLE

OPEN ACCESS Check for updates

Vacuum infiltration of biobased and synthetic polymers for enhancing wood properties in construction

Maria Naissi, Andrija Pranjic, Steliyana Yancheva and Martin Trautz

Chair of Structures and Structural Design (trako), RWTH Aachen University, Aachen, Germany

ABSTRACT

This research focused on enhancing the structural performance of untreated wood for potential structural applications through polymer infiltration. Three infiltration substances - methyl methacrylate resin (TT_a, TT_b), stabilizing resin (S17) and gelatine (Ga_M), and a control group of untreated raw wood were tested. The process combined in-situ polymerization with vacuum stabilization at −95 kPa, allowing deep polymer penetration. TT_B achieved the highest penetration by weight ($P_w \approx 63\%$). Mechanical characterization included compressive strength, stiffness, relative water absorption, density changes, biodegradability, and scanning electron microscopy (SEM) analysis. Due to high preparation effort, small specimens' sizes (n = 4–8) were used, with T-tests for statistical evaluation. Infiltration with TT_b increased the compressive strength of wood parallel to the grain by 33% (p = 0.029) and the stiffness by 21% (p = 0.047). Perpendicular to the grain, stiffness rose 2.8-fold (p = 0.082), and ductility improved 1.5-fold (p = 0.001) compared to raw wood. SEM confirmed polymer deposition in the lumen structure. These findings demonstrate the potential of vacuum polymer infiltration, to enhance untreated wood's mechanical properties. Further research is needed to refine polymer formulations, test long-term durability, and evaluate the environmental and economic feasibility of implementing this technology on a larger scale.

ARTICLE HISTORY
Received 4 March 2025
Revised 25 May 2025
Accepted 7 June 2025

KEYWORDS
Wood vacuum stabilization; load bearing construction; gelatine; methyl methacrylate resin; compression strength; stiffness

Introduction

While polymer infiltration has been widely explored as a means to improve the mechanical and environmental durability of wood, many existing treatments face challenges such as uneven distribution of the infiltrate, limited penetration depth, or insufficient long-term performance under environmental stressors (Lemaire-Paul *et al*. 2023, Augustina *et al*. 2024). This study investigates the potential of vacuum-assisted infiltration using both synthetic and bio-based polymeric resins, aiming to overcome these limitations by achieving deeper, more uniform integration into the wood matrix.

The stabilization of untreated wood through an infiltration is a method to enhance its mechanical, physical, and chemical properties. The research focused on improving the properties of wood as a construction material, specifically for load-bearing building applications. Untreated wood is susceptible to structural stresses and environmental impacts such as moisture, biological degradation, thermal effects, and weathering. These limitations are addressed through the adaptation of raw wood by infiltrating the wood matrix under vacuum with a synthetic and bio-based polymeric resin. The curing of these substances results in a stabilization effect, leading to an improved construction material while keeping the wood's original dimensions. Boonstra (2016) and Schneider (1994) have described such method, emphasizing the significant steps in producing wood polymer composites (WPC), where solid wood is impregnated with a polymerizable monomer or prepolymer. Comparative analysis in this paper shows a significant difference between untreated and infiltrated wood. In industrial applications this technique of enhancing wood properties is already established, such cases are furniture production and flooring for both interior and exterior use.

Commercial applications predominantly rely on synthetic polymers to produce WPC (Patachia and Croitoru 2016, Hunt and Dunky 2023). Nevertheless, the possibility of replacing conventional synthetic polymers with bio-based alternatives has been demonstrated by the results. Compared to untreated wood, the bio-based wood composite exhibits improved stability, durability, and resistance to environmental factors. Although bio-based wood achieves similar compression strength and biodegradability to synthetic composites, it still presents weaknesses in water absorption, which are being further examined in ongoing research. The choice of construction material plays an important role in the context of climate-resilient construction and reducing environmental impact, such as the mitigation of fine particulate pollution and reducing climate-damaging emissions.

The effectiveness of infiltration depends on various parameters, including the porosity of the wood species, the viscosity and reactivity of the infiltrate, and processing conditions such as pressure, temperature, and curing time.

CONTACT Maria Naissi naissi@trako.arch.rwth-aachen.de Chair of Structures and Structural Design (trako), RWTH Aachen University, Schinkelstr. 1, Aachen 52062, Germany

This study explores the mechanisms, materials, and optimization strategies involved in wood stabilization through infiltration. By understanding the interactions between infiltrates and wood microstructures, in order to achieve an improved wood material for industrial and structural applications.

The conducted research comprises a comprehensive evaluation of the effects of polymer infiltration on wood properties through a series of analytical and mechanical tests. Penetration was quantified by calculating the uptake of the infiltrate within the wood structure. Compression testing was performed with respect to the wood's grain direction, accompanied by an analysis of frequently occurring failure modes to assess structural integrity. The bulk density of the resulting wood polymer composite (WPC) was determined to evaluate the material's consolidation. Scanning Electron Microscopy (SEM) was employed to visually assess the degree of infiltration and the distribution of the polymer within the wood matrix. Furthermore, comparative analyses were conducted on water absorption behaviour and biodegradability. The latter included a visual inspection of colour changes in the wood core, serving as an indicator of microbial activity and material degradation over time.

State of the art

Research on the enhancement of the wood matrix was conducted by Wehsener *et al*. (2023) who explored the delignification and densification of wood. He finds out that by removing 90% of the lignin, the bending strength and dimensional stability are improved. Lemaire-Paul *et al*. (2023) demonstrated that using a high vacuum pressure (−90 kPa) to infiltrate silicon dioxide improves the wood density, reduces porosity, and lowers water absorption. Additionally, he noted that the method of high-pressure vacuum impregnation enhances creep resistance in spruce wood.

The influence of the synthetic infiltration material on wood was analysed by Stefanowski *et al*. (2018) who identified low molecular weight [phenol formaldehyde] PF, [melamine] MF, and [dimethydihydroxyethyleneurea] DMDHEU resins as effective for stabilization. Behr (2020) and Bicke (2019) showed that MF and PF resins improve hardwood properties and laminated veneer lumber, but issues with self-condensation and diffusion persist. Though using the vacuum-pressure impregnation the importance of an optimal drying process for the wood specimens needs to be considered.

Following the aim of reducing climate warming driving agents (e.g. greenhouse gases (GHGs), volatile organic compounds (VOCs), aerosol emissions), in the past years there has been an increasing interest in research on bio-based infiltration, such as Hunt and Dunky (2023) escribing the establishment of bio-based engineered wood products (EWPs) in the market. There are promising opportunities for bio-based substances used as adhesives in wood enhancement. They mention lignin-based adhesives as an example, which can partially replace PF resins but lack moisture resistance and economic feasibility. They describe applications like interior panels, cross-laminated timber, and particleboards. But the transfer into construction fails because of the lack of large-scale technique, stricter structural requirements, practice and limited workforce expertise. Besides, Patachia and Croitoru (2016) identified biopolymers, including polysaccharides and proteins, as promising but highlighted variability in results. Advanced methods like biopolymer hydrogels and ionic liquids for enhanced penetration are being explored. There is a growing interest in using gelatine-based enhancements as a bio-based alternative. Naïssi *et al*. (2024) identified gelatine as a potential material for membranes with properties comparable to polyethylene (PE) and polyvinylchlorid (PVC). Additives like beeswax and soy protein improve gelatine's stability in humid conditions. Kolbe *et al*. (2023) achieved promising shear strength with gelatine in Glued-in Rods (GiR), while Goldhahn *et al*. (2020) observed meniscus-like gelatine films within wood that impede water transport. Dorr *et al*. (2015) showed that 40% gelatine formulations outperformed synthetic adhesives in select tests, with tannin reducing moisture absorption.

The current state of the art in wood stabilization research demonstrates a fragmented approach, influenced by variables such as wood type, applied substances, testing methodologies, industrial practices, and application goals. A significant portion of research remains focused on micro-level phenomena, lacking standardized investigations into the blocking behaviour of substances within the wood's voids, which is critical for ensuring uniform material production. Furthermore, even under consistent testing conditions, the natural variability of wood and other bio-based substances often results in substantial discrepancies in outcomes. This illustrates the challenge of standardization in wood stabilization.

Degree of stabilization

The degree of wood stabilization is influenced by the cell wall components (cellulose, lignin, and hemicellulose), wood moisture and in general the wood species. Besides, influenced by the bulk density of the wood, a pore volume of approximately 50–60% can be observed (Niemz and Sonderegger 2021). This high porosity plays a significant role in the infiltration process, affecting the distribution and depth of penetration of stabilizing substances. Schneider (1994) examines substances used to utilize the wood polymer composites (WPC) and to enhance the wood density. He found out that the bonding mechanisms vary, with phenol-formaldehyde penetrating the wood cell walls and vinyl compounds typically filling the cell lumens. Besides, the lower density of softwood likely requires more infiltration material to achieve properties like those of hardwood. However, due to the local availability and economic considerations, softwood has been selected as the focus of this research.

The vacuum stabilization process is a method that enhances the strength, durability, or resistance to environmental factors of wood. It is a physicochemical method, as no chemical reactions occur between the wood and polymer (except during polymer curing), but the physical structure of the wood is altered to allow deep penetration of the polymer into the wood fibres. In this process, wood is subjected to a vacuum treatment that removes air from the wood's pores, creating space for polymer absorption. The polymer is introduced under vacuum, ensuring deep penetration into the fibres.

Afterward, the polymer is cured forming a permanent bond with the wood.

Synthetic Polymers are artificially produced plastics widely used in civil engineering applications, especially where high load-bearing capacity and durability are essential. Examples include bridges, facades, and outdoor load-bearing components. In this research, resins and acrylic resins were applied to the wood matrix. Synthetic polymers in the vacuum-pressure method, used for WPC production, are classified into polymerizable monomers and prepolymers (Schneider 1994). Bio-based Polymers on the other side, derived from renewable raw materials, offer comparable properties to synthetic polymers with a reduced environmental footprint. Unlike synthetic polymers, they are not polymerizable monomers but belong to natural polymers, consisting of long amino acid chains.

Polymer viscosity is an important factor influencing infiltration into the wood matrix. Low- and medium-viscosity polymers are easily introduced through pressure and vacuum, whereas high-viscosity polymers rely on flow and diffusion-displacement mechanisms for infiltration. Furthermore, non-swelling polymers remain confined to the cell lumens after infiltration. In contrast, swelling polymers with low molecular weight penetrate the wood structure, causing the wood cell walls to swell during curing. This cell-wall phenomenon significantly enhances the wood's stability compared to cell-lumen WPC (Schneider 1994).

Materials and methodology

To evaluate and describe used materials properties and methodology in this study, standardized testing procedures are outlined in DIN EN 15534-1: 2018-02, which provides comprehensive methods for characterizing wood-polymer composites (WPC) and natural fibre composites (NFC). In addition to the testing procedures, the study utilized the guidelines of DIN CEN/TS 15534-2: 2007 to ensure a detailed description of the infiltration substances under investigation. This combined approach allowed for a comprehensive evaluation of the material's properties.

It is important to note that this study represents an early-stage investigation focused on the material-level performance of untreated wood modified through polymer infiltration. As such, the experimental work was limited in several respects like sample sizes were limited ($n = 4$–8), SEM analysis was used qualitatively to confirm infiltration, without depth quantification. Life cycle assessment and structural-scale implementation were beyond the current scope. These limitations constrain generalization but provide a basis for future research focused on formulation refinement and knowledge of the functional contribution of each substance in wood.

Material: substances used for infiltration

The selected substances were chosen for their ability to enhance the mechanical properties of wood. These materials undergo a curing process after infiltration, transitioning to a stable, durable state. Curing stabilizes the wood structure, improving its resistance to mechanical stress, moisture, temperature fluctuations, and microbial attack. By deeply penetrating and polymerizing within the wood matrix, these substances provide long-term reinforcement and protection, making them highly effective for wood stabilization applications. Two conventional synthetic substances were selected as benchmarks for comparative analysis. These materials serve as points of reference to evaluate the bio-based alternative's performance, infiltration efficiency, and curing behaviour. By comparing their mechanical reinforcement properties and environmental resistance, the study aims to identify the advantages and limitations of the bio-based material relative to established synthetic solutions. This approach provides a comprehensive assessment of the material's potential for wood stabilization and its suitability for sustainable applications.

Methacrylate resin (TT_a, TT_b)

Based on the findings of Neyses *et al*. (2017) and Rui *et al*. (2019), the suitability of methyl methacrylate resin (TurnTex, MMA) for wood stabilization is well-demonstrated. The resin is specifically designed to deeply penetrate wood pores, stabilizing the structure upon curing. It exhibits a low dynamic viscosity of less than 4–6 mPas, allowing it to easily infiltrate even fine cracks and small pores under vacuum conditions. The polymerization process involves crosslinking triggered by the application of a hardener and subsequent heating, in that case, an oven was used. During curing, the resin forms a robust bond with the cellular structure of the wood, significantly enhancing its dimensional stability, resistance to moisture, and mechanical durability. The curing process was conducted at an oven temperature of 90°C, following a stepwise heating protocol, due to the absence of standardization for this procedure. The temperature was increased incrementally in 10-minute intervals, with samples exposed to 60°C, 70°C, and 80°C for 10 min each before being held at 90°C for the remaining duration of the process. Samples from group TT_a were maintained at 90°C for 30 min, while those from group TT_b were subjected to 90°C for 60 min. This approach ensured gradual temperature acclimatization and allowed for comparative analysis of the curing duration's impact on material properties. The stepwise heating process aimed to optimize the curing efficiency while minimizing potential thermal stresses on the wood samples.

Stabi 17 resin (S17)

Based on the findings of *Stabi 17 B*, the suitability of a resin with a medium dynamic viscosity is stated and well researched for wood stabilization. Due to the properties, it requires either extended infiltration time or stronger vacuum pressure to achieve effective penetration into wood matrix. It undergoes a polymerization upon the addition of a hardener, forming a solid and robust polymer structure, but the curing process takes place naturally, under air conditions. While it exhibits good adhesion to wood, its penetration performance may be limited to dense wood species or fine pores, where achieving uniform distribution could be challenging.

Gelatine (Ga_M, Ga_M_f)

Based on the findings of Dorr *et al*. (2015); Goldhahn *et al*. (2020); Kolbe *et al*. (2023); Naïssi *et al*. (2024) and Patachia

and Croitoru (2016), gelatine, a biopolymer derived from the collagen fibres of animal origin, demonstrates characteristics that distinguish it from synthetic resins. As a natural polymer, gelatine consists of long chains of amino acids, making it a protein-based material. In terms of viscosity and penetration, gelatine exhibits high dynamic viscosity of around 1200 mPas, particularly at higher concentrations, which limits its ability to penetrate fine pores or dense woods. It is more suitable for open-pored woods or larger cracks. Unlike synthetic resins, gelatine does not undergo chemical curing but rather forms a gel upon cooling. This stabilization is reversible, as gelatine reverts to its liquid state when exposed to heat or moisture, significantly limiting its long-term effectiveness. Furthermore, its natural origin and biodegradability are advantageous compared to synthetic alternatives. The specimens were prepared with two distinct formulations to evaluate the effects of varying gelatine and glycerine concentrations: Ga_M samples contained 16% gelatine and 5% glycerine, emphasizing a higher protein content for potential stabilization effects. Ga_M_f samples contained 5% gelatine and 16% glycerine, prioritizing plasticizing properties to assess flexibility and penetration characteristics. These formulations were designed to investigate the influence of the gelatine-to-glycerine ratio on the mechanical and physical properties of the treated wood, providing insights into the role of each component in the stabilization process.

Material: stability of spruce wood

The specimens were cut from a glulam beam, class Gl24 (according to the DIN EN 14080 standard). The density of the raw spruce wood ranged between 350–400 kg/m^3, with an average value of 384 kg/m^3. It was selected as the base material due to its availability and favourable characteristics, including its uniform grain structure and widespread application in wood studies. The wood samples were prepared in dimensionally identical pieces measuring $20 \times 20 \times 30$ mm. To minimize potential changes in the wood's properties, all samples were processed within 24 h of cutting. At the time of preparation, the mean moisture content of the wood was 8%. The samples were oriented both parallel and perpendicular to the grain, with each containing at least five lamellae per specimen, ensuring the samples were free from defects such as knots, branch junctions, or resin-based adhesive seams, providing consistent material properties for testing.

The experiments were conducted under controlled laboratory conditions at 20°C and a relative humidity of 60%, ensuring stable environmental factors throughout the study. These conditions were maintained to minimize external influences on the wood's physical and mechanical properties during testing.

Methodology: vacuum stabilization process

In preparation for the vacuum stabilization process, wood samples are cut to required shapes, placed in a plastic tray with space between them and weight placed on top, preventing an uptake of the specimens, and covered with solution. The tray is then positioned in the vacuum chamber. The vacuum pump is activated until the maximum vacuum level is achieved, depending on the viscosity of the substance. For methacrylate resin (TT_a) the vacuum pressure was maintained between 91.4 and 94.8 kPa for a duration of 30 min, and for methacrylate resin (TT_b) a constant vacuum pressure of 91.4 kPa was applied for 30 min. Specimens with stabilizing resin were subjected to a vacuum pressure of 91.4 kPa for 30 min. For gelatine-based samples (Ga_M, Ga_M_f) the vacuum pressure ranged from 89.7 to 91.4 kPa, with a duration varying between 30 and 55 min. Extracting the trapped air from the wood matrix and allowing the solution to infiltrate. This is indicated by bubble formation, which ceases once oxygen is fully removed. The vacuum is then gradually released. Samples, now solution-saturated, are left to dry and cure naturally until weight stabilizes (∼2 weeks). For curing solutions, samples are oven-cured at a gradually increasing temperature (90°C) to prevent deformation. After curing, samples are ready for use.

Experimental studies

Study: resin uptake calculation

To ascertain the success of the method the amount of resin uptake is calculated. Calculations are based on Hartig *et al*. (2023), which basically envisages different densities before and after infiltration of the specimen.

The specimens were weighed before and up to two weeks after the vacuum stabilization process (during the preparation process, it has been found that the weight has stabilized after an average of two weeks). The variability of the wood is considered by determining the densities specifically for each test specimen. For a generally valid assertion, an averaged trend line was determined from the results.

The specific density of wood before infiltration is calculated:

$$\rho_{\text{wood}} = m_{\text{wood}}/V \tag{1}$$

m_{wood} is the mass of wood and V is the volume of wood before infiltration.

The specific density of wood after infiltration is calculated:

$$\rho_{\text{wood + inf}} = m_{\text{inf}}/V \tag{2}$$

m_{inf} is the mass of infiltration wood.

The specific amount of resin within the wood volume is calculated:

$$\rho_{\text{inf/wood}} = (m_{\text{inf}} - m_{\text{wood}})/V \tag{3}$$

The theoretically maximum amount of resin within the wood is calculated:

$$\rho_{\text{inf/wood,max}} = \rho_{\text{inf}}(1 - \rho_{\text{wood}}/\rho_{\text{cell wall}}) \tag{4}$$

$\rho_{\text{inf,TT}} = 1050$ kg/m^3; $\rho_{\text{inf,S17}} = 903$ kg/m^3; $\rho_{\text{inf,Ga\_M}} = 1050$ kg/m^3; $\rho_{\text{inf,Ga\_M\_f}} = 1040$ kg/m^3; $\rho_{\text{cell wall}} \approx 1500$ kg/m^3 (Matejak and Kozakiewicz 2011).

The difference between the actual – and the theoretical absorption is defined with the penetration calculation P_w which is based on Tondi *et al*. (2012). It should be noted that the values represent the substance embedded with the wood specimen. There is no differentiation between internal infiltration and external adhesion.

The specific penetration by weight (P_w) is calculated:

$$P_w = \rho_{\text{inf/wood}} / \rho_{\text{inf/wood,max}} \quad (5)$$

Study: determination of ultimate strength in non-buckling compression parallel and perpendicular to grain and determination of the density

The German standards DIN 52185: 1976-09 specify testing methods for assessing wood strength parallel to the grain (PARA), and DIN 52192: 1979-05 specify testing methods for assessing wood strength tangential to the grain (SENK). Respectively, DIN EN 408: 2012-10 outlines procedures for determining the physical and mechanical properties of structural wood and glued laminated timber.

The compression tests were conducted using the Universal Testing Machine 112 from TesT GmbH, with a maximum load capacity of 50 kN. The specimens measuring $30 \times 20 \times 20$ mm ($b \times t \times h$), are placed vertically between two steel plates, with its longitudinal axis aligned along the loading axis. The experiment was conducted on 56 small, defect-free wooden blocks from a single wood species. They were categorized based on treatment, as outlined in Table 1. The following baseline settings were applied depending on the specimen's series:

Table 1. Overview of tested specimens for the compression test.

Specimen	Label	Grain	Weight		Oven-time	ρ, **ρ (infiltrated)**	P_w
			Infiltrated [g]	Increase [%]	[h]	[kg/m^3]	[%]
Raw	CS_C1_P1_111	perpendicular	–	–	–	287	–
	CS_C1_P1_112	perpendicular	–	–	–	483	–
	CS_C1_P1_113	perpendicular	–	–	–	279	–
	CS_C1_P1_114	perpendicular	–	–	–	374	–
	CS_C1_P1_125	parallel	–	–	–	340	–
	CS_C1_P1_126	parallel	–	–	–	278	–
	CS_C1_P1_127	parallel	–	–	–	344	–
	CS_C1_P1_128	parallel	–	–	–	308	–
Ga_M	CS_C1_P2_49	perpendicular	5.9	113	–	**491**	8
	CS_C1_P2_50	perpendicular	5.8	115	–	**483**	9
	CS_C1_P2_51	perpendicular	6.3	106	–	**526**	5
	CS_C1_P2_52	parallel	5.2	108	–	**436**	5
	CS_C1_P2_53	parallel	5.2	106	–	**436**	4
	CS_C1_P2_54	parallel	6.0	106	–	**497**	4
	CS_C1_P2_55	parallel	5.3	107	–	**441**	4
	CS_C1_P2_57	perpendicular	4.4	139	–	**368**	8
	CS_C1_P2_58	perpendicular	6.2	142	–	**519**	11
	CS_C1_P2_59	perpendicular	4.4	133	–	**364**	2
	CS_C1_P2_65	parallel	5.6	125	–	**468**	8
	CS_C1_P2_66	parallel	5.3	121	–	**444**	7
	CS_C1_P2_138	parallel	7.2	118	–	**446**	6
	CS_C1_P2_142	perpendicular	9.6	125	–	**587**	9
Ga_M_f	CS_C1_P2_41	parallel	6.0	111	–	**498**	7
	CS_C1_P2_42	parallel	5.7	108	–	**478**	5
	CS_C1_P2_45	parallel	5.0	107	–	**418**	3
TT_a	CS_C1_P3_72	perpendicular	9.3	211	1.0	**775**	50
	CS_C1_P3_73	perpendicular	9.0	209	1.0	**749**	47
	CS_C1_P3_74	parallel	7.4	190	1.0	**613**	37
	CS_C1_P3_75	parallel	7.2	187	1.0	**597**	35
	CS_C1_P3_98	perpendicular	9.1	196	1.0	**760**	48
	CS_C1_P3_99	perpendicular	7.8	170	1.0	**650**	34
	CS_C1_P3_100	parallel	6.4	175	1.0	**537**	27
	CS_C1_P3_101	parallel	9.1	185	1.0	**755**	45
	CS_C1_P3_102	parallel	6.3	127	1.0	**523**	15
	CS_C1_P3_103	parallel	5.8	170	1.0	**479**	23
	CS_C1_P3_104	perpendicular	9.0	190	1.0	**746**	46
	CS_C1_P3_105	perpendicular	7.7	168	1.0	**638**	33
	CS_C1_P3_106	parallel	6.3	169	1.0	**523**	26
	CS_C1_P3_108	parallel	6.3	169	1.0	**526**	26
TT_b	CS_C1_P3_147	perpendicular	8.1	137	1.5	**674**	26
	CS_C1_P3_148	perpendicular	7.8	139	1.5	**649**	25
	CS_C1_P3_149	perpendicular	8.8	186	1.5	**730**	44
	CS_C1_P3_150	perpendicular	6.4	137	1.5	**537**	19
	CS_C1_P3_151	parallel	7.6	136	1.5	**634**	23
	CS_C1_P3_153	parallel	6.7	136	1.5	**557**	19
	CS_C1_P3_155	parallel	8.3	170	1.5	**693**	37
	CS_C1_P3_156	parallel	6.5	172	1.5	**545**	28
S17	CS_C1_P2_81	perpendicular	5.4	118	–	**451**	9
	CS_C1_P2_82	perpendicular	5.0	113	–	**413**	7
	CS_C1_P2_83	parallel	3.9	116	–	**323**	6
	CS_C1_P2_84	parallel	6.8	116	–	**564**	10
	CS_C1_P2_86	parallel	6.0	115	–	**501**	8
	CS_C1_P2_87	perpendicular	5.8	112	–	**317**	5
	CS_C1_P2_88	perpendicular	5.3	118	–	**439**	9
	CS_C1_P2_91	parallel	4.6	117	–	**384**	7
	CS_C1_P2_92	parallel	5.6	114	–	**308**	5

Table 2. Overview of tested specimens for the microscopic analysis.

Specimen	Label	Grain	Weight		Oven-time [h]	ρ, $\boldsymbol{\rho}$ **(infiltrated)** [kg/m^3]	P_w [%]
			Infiltrated [g]	Increase [%]			
Raw	CS_C1_P1_136	parallel	–	–	–	337	–
Ga_M	CS_C1_P2_140	parallel	5.4	121	–	**450**	7
TT_a	CS_C1_P3_24	perpendicular	10.6	226	1.0	**883**	63
TT_b	CS_C1_P3_145	perpendicular	6.6	140	1.5	**548**	20
S17	CS_C1_P2_10	perpendicular	5.6	144	–	**467**	20

- Serie PARA: Specimens tested parallel to the grain with a test speed of 2 mm/min until a maximum peak drop of 20%.
- Serie SENK: Specimens tested perpendicular to the grain with a test speed of 2 mm/min until a displacement of 15 mm was reached.

Study: SEM microscopic analysis and biodegradability determination

SEM microscopic analysis

A tabletop scanning electron microscope (SEM, EM-30N, COXEM) was utilized to investigate the microstructural changes within the wood induced by the stabilizing substances. The wood composite specimens (Table 2) were sectioned into smaller pieces to facilitate detailed analysis of the penetration depth and distribution of the substances within the wood matrix. Due to the higher viscosity and for that reason the required stronger vacuum pressure, specimens with gelatine as infiltration material were emphasized to measure the effectiveness of infiltration. SEM imaging provided insights into the extent of substance penetration, including whether the gelatine adhered to the cell walls or accumulated within the cell lumens. This created a first understanding about the efficiency of the stabilization process and the challenges associated with high-viscosity materials like gelatine.

Biodegradability determination

The separation of the wood-composite in its individual components and the opportunity of biodegradation as a natural process need to be understood before a material enters the market for construction material. The aim is to achieve a controlled separation of the primary components over a specific time. Since the biodegradation of wood is influenced by different environmental conditions, such a process especially for untreated wood in construction, cannot be excluded and may cause premature failure. The modification of wood is a method of protecting its stature and thus its properties (Sandberg *et al*. 2021). While wood itself is naturally biodegradable, the incorporation of infiltration (polymers, resin or chemicals) can alter its degradation behaviour, potentially leading to the persistence of non-biodegradable residues or microplastics, eventually leaving a certain environmental impact.

The evaluation and implementation of biodegradability for WPCs are based on DIN EN 15534-1: 2018-02. Four specimens were tested: one untreated specimen (raw) as a reference, and three infiltrated specimens with bio-based and synthetic materials (Table 3). The specimens were buried in soil for 10 weeks under natural environmental conditions to simulate outdoor exposure. The state and condition are analysed visually. First the surface of the material and secondly the depth of biodegradation recognized by the change in colour were determined by cutting the WPC into four pieces.

Study: relative water absorption

Moisture content was determined according to DIN 52183: 1977-11 using Equation (6):

$$\mathrm{MC} = \frac{W_{\mathrm{wet}} - W_{\mathrm{dry}}}{W_{\mathrm{dry}}} \tag{6}$$

The standard describes a method that determines the percental moisture content based on the ratio between the mass of water contained in the wood sample water and the mass of the water-free (kiln-dry) wood sample. Water soaking tests were conducted to evaluate the behaviour of treated specimens in a high-humidity environment. Six specimens per substance, oriented both parallel and perpendicular to the grain, as well as untreated controls, were included (Table 4). Initial dry weights and moisture contents were recorded for each specimen. Subsequently, specimens were immersed in distilled water for 24 h at room temperature. Post-soaking, weight and moisture content increases were measured. Following a 24-h drying period under ambient conditions, final weight and moisture content were recorded to assess any residual effects of water immersion.

Results

Results: resin uptake calculation

The actual amount of resin absorbed in the wood differs from the theoretical maximum calculation, with TT_a and TT_b

Table 3. Overview of tested specimens for the determination of the biodegradability.

Specimen	Label	Grain	Weight		Oven-time [h]	ρ, $\boldsymbol{\rho}$ **(infiltrated)** [kg/m^3]	P_w [%]
			Infiltrated [g]	Increase [%]			
Raw	CS_C1_P1_115	perpendicular	–	–	–	382	–
Ga_M	CS_C1_P2_63	perpendicular	5.3	138	–	**444**	11
TT_a	CS_C1_P3_97	perpendicular	6.1	167	1.0	**508**	24
S17	CS_C1_P2_79	perpendicular	4.9	113	–	**406**	6

Table 4. Overview of tested specimens for the relative water absorption test.

Specimen	Label	Grain	Weight		Oven-time [h]	ρ, **ρ (infiltrated)** [kg/m^3]	P_w [%]
			Infiltrated [g]	Increase [%]			
Raw	CS_C1_P1_118	perpendicular	–	–	–	473	–
	CS_C1_P1_119	perpendicular	–	–	–	458	–
	CS_C1_P1_120	perpendicular	–	–	–	303	–
	CS_C1_P1_133	parallel	–	–	–	386	–
	CS_C1_P1_134	parallel	–	–	–	282	–
	CS_C1_P1_135	parallel	–	–	–	280	–
Ga_M	CS_C1_P2_47	perpendicular	5.9	111	–	**493**	7
	CS_C1_P2_56	parallel	5.9	110	–	**490**	7
	CS_C1_P2_61	perpendicular	5.3	125	–	**442**	8
	CS_C1_P2_62	perpendicular	6.1	155	–	**506**	12
	CS_C1_P2_64	parallel	6.6	121	–	**550**	8
	CS_C1_P2_139	parallel	5.5	123	–	**460**	7
TT_a	CS_C1_P3_69	perpendicular	8.0	187	1.0	**668**	37
	CS_C1_P3_70	perpendicular	5.7	172	1.0	**473**	22
	CS_C1_P3_76	parallel	8.9	221	1.0	**742**	50
	CS_C1_P3_77	parallel	7.9	221	1.0	**658**	42
	CS_C1_P3_96	perpendicular	6.9	148	1.0	**577**	24
	CS_C1_P3_107	parallel	6.2	168	1.0	**518**	25
S17	CS_C1_P2_80	perpendicular	5.2	111	–	**433**	6
	CS_C1_P2_85	parallel	6.9	119	–	**573**	12
	CS_C1_P2_89	perpendicular	5.5	118	–	**455**	9
	CS_C1_P2_90	perpendicular	4.2	113	–	**347**	5
	CS_C1_P2_93	parallel	4.7	116	–	**392**	7
	CS_C1_P2_94	parallel	4.3	114	–	**359**	6

getting the closest to theory. Similar divergences are also documented in Hartig *et al*. (2023). The highest increase in density of infiltrated wood is achieved by TT_a. The values of P_w show that none of the specimens is completely petrified. The best values are achieved by infiltration with MMA, with a maximum value of 63%. Only a few composites with S17 and gelatine achieved values above 10%. Results with the perpendicular to grain achieve higher values. Optimization of the stabilization process could increase the P_w. This includes extending the time of the vacuum process, increasing the vacuum pressure, or varying the substance, possibly focusing on substances with lower viscosities (Figure 1).

Results: determination of ultimate strength in non-buckling compression parallel and perpendicular to grain and determination of the density

Failure modes

During non-buckling compression tests on stabilized and raw wooden blocks (30 × 20 × 20 mm), distinct failure mechanisms were identified depending on the direction of compression relative to the timber grain. When compressed parallel to the grain, most specimens failed predominantly due to the crushing of the timber's cellular structure (Figure 2, left), a mode characterized by localized collapse and densification of wood fibres. In some cases, additional failures such as splitting, where cracks propagate along the grain (Figure 2, mid-left), end rolling caused by instability at specimen edges (Figure 2, mid-right), and shearing along weaker planes further contributed to the overall damage.

Compression perpendicular to the grain exhibited mostly compaction primary failure mode (Figure 2, right), leading to grain slipping and wrinkling, where the wood's layered structure deformed and shifted under pressure. This mode reflects the lower strength and stiffness of wood in this orientation. Occasionally, delamination occurred, where the layers of wood separated due to stresses exceeding the adhesive or cohesive forces within the material.

Compression test

The comparison of mean values for all specimens is illustrated in Figure 3 for both the PARA and SENK series. Table 5 presents the mean values for stiffness [$F_{\text{max, mean}}$ (N/mm)], maximum force [$F_{\text{max, mean}}$ (N)], ductility [$D_{\text{rel,u}}$ (–)] and mean density [ρ_{mean} (kg/m^3)] with corresponding p-values acquired with T-test. For certain test series, p-values exceeded the conventional threshold of 0.05, which may be attributed to the small specimen sizes ($n = 4$–8) and inherent variability of the wood material. While statistical significance was not achieved in these cases, observable trends and effect sizes still provide meaningful insight into the influence of the treatment. Based on the statistical evaluation, the TT_B series exhibited the most consistent performance across specimens in parallel and perpendicular, while the S17 series showed the greatest variation in results.

For specimens oriented parallel to the timber grains, the maximum force can be identified from the force-deformation diagram. Notably, specimens Ga_M_f and TT_b exhibited longer yielding curve behaviour after reaching their initial maximum force. This was followed by a secondary increase in force, with mean curves indicating an additional peak at approximately 13% strain for Ga_M_f and 20% strain for TT_b (see Figure 3, left). For clarity and consistency in Table 5, only the first maximum force prior to yielding is considered for comparison.

For the SENK series, where the specimens are oriented perpendicular to the timber grains, the maximum force (maximum bearing strength) is determined using the 2% offset method (see Figure 3, right). This approach identifies yielding when the deformation exceeds 2% (similarly is defined in EN 408 to

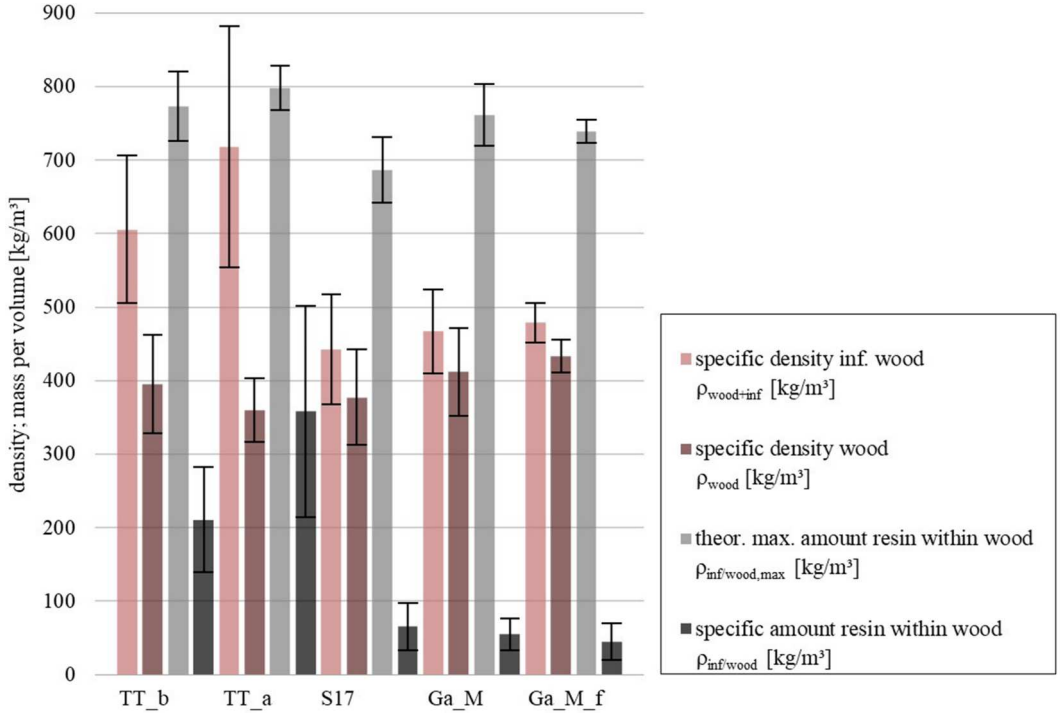

Figure 1. Comparative mean densities of wood, resin, theoretical – and actual amount of infiltration within the wood specimen. The error bars correspond to the standard deviation of the measured values. The error bars correspond to the standard deviation of the measured values, illustrating the degree of variability among the specimens tested.

Figure 2. Typical failure mode occurred during compression tests. Left: crushing failure of raw spruce specimen (CS_C1_P1_126); Mid-left: crushing and splitting failure of Ga_M (CS_C1_P2_54); Mid-right: end rolling, crushing and splitting failure of Ga_M_f (CS_C1_P2_41); Right: compaction and wrinkling of raw specimen (CS_C1_P1_111).

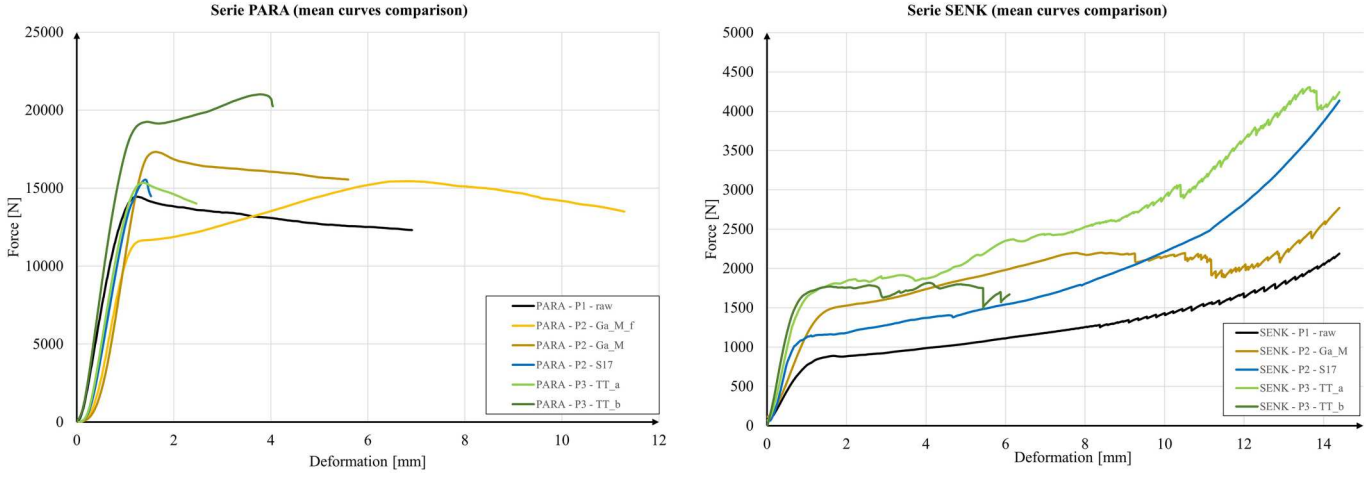

Figure 3. Mean force–deformation curves of all specimens in: Left – parallel to grain series PARA; Right – perpendicular to the grain series SENK.

Table 5. Mean values of compression test results.

Grain	Substance	$F_{max,\ mean}$ [N]		K_{mean} [N/mm]		D [–]		ρ_{mean}, $\boldsymbol{\rho_{mean}}$ **(infiltrated)** [kg/m^3]
Parallel	RAW	14,472		17,640		2.49		317.5
(PARA)	Ga_M_f	11,644	(0.057)	14,490	(0.040)	1.96	(0.024)	**464.7**
	Ga_M	17,713	(0.031)	17,014	(0.549)	1.85	(0.002)	**452.6**
	S17	16,103	(0.528)	16,983	(0.772)	1.98	(0.012)	**416.0**
	TT_a	15,416	(0.480)	19,665	(0.121)	2.49	(0.994)	**569.1**
	TT_b	19,389	(0.029)	21,339	(0.047)	2.37	(0.414)	**607.3**
Perpendicular	RAW	878		927		2.24		355.8
(SENK)	Ga_M	1485	(0.007)	1412	(0.040)	2.04	(0.544)	**476.9**
	S17	1154	(0.101)	1669	(0.083)	2.27	(0.958)	**405.0**
	TT_a	1773	(0.052)	2056	(0.003)	1.97	(0.352)	**719.7**
	TT_b	1739	(0.128)	2583	(0.082)	3.44	(0.001)	**647.5**

Note: The values in brackets representing *p*-value acquired in *t*-test.

estimate compressive strength) which for these specimens corresponds to a displacement of 0.6 mm offset. In timber, this method is mostly used for fasteners (Smith and Foliente 2002), but here is taken for comparison purposes. The resulting maximum force occurs then at 5–10% strain. Relative ductility, which provides a comparative measure of ductility across specimens, is calculated using Equation (7). It is defined in Swiss code for timber structures SIA 2003: 2003 and European code EN 12512: 2001.

$$D_{rel,u}\ [-] = \frac{u_u}{u_y} \tag{7}$$

The ultimate deformation is defined at the point of maximum force, while the yield deformation (elastic boundary) is determined using the Karacabeyli and Ceccotti method (Forintek) (Karacabeyli and Ceccotti 1996). This method identifies the onset of timber yielding as the displacement at 50% of the maximum force (see Figure 4, left).

Initial axial stiffness is calculated according to Equation (8), taking part of the curve where capacity is from 10% to 40%, based on DIN EN 26891: 1991-07, like in Egner and Dietsch (2024).

$$K\ [\mathrm{N/mm}] = \frac{0.4 \cdot F_{max} - 0.1 \cdot F_{max}}{u(0.4 \cdot F_{max}) - u(0.1 \cdot F_{max})} \tag{8}$$

The comparison of the PARA series, as shown in Figure 3 and Table 5, reveals varied mechanical responses depending on the type of infiltrated polymer used, in contrast to the raw wood specimens represented by the black curve. The force-deformation diagrams, as well as mean curves, of all specimens are shown in Figure 5 (PARA serie) and Figure 6 (SENK serie). The Ga_M series (gold curve) showed mechanical behaviour similar to the raw wood, with stiffness values remaining consistent while achieving a strength increase of approximately 22%. This improvement, however, slightly reduced the relative ultimate ductility of the specimens. In contrast, the Ga_M_f series (yellow curve) demonstrated high ductility, with the ability to reach an additional strength peak after yielding. Despite having only 80% of the strength (first maximum) and stiffness of the raw specimens, the failure modes significantly changed, with specimens failing through a combination of end rolling, crushing, and splitting. The S17 series (blue curve) presented brittle behaviour during

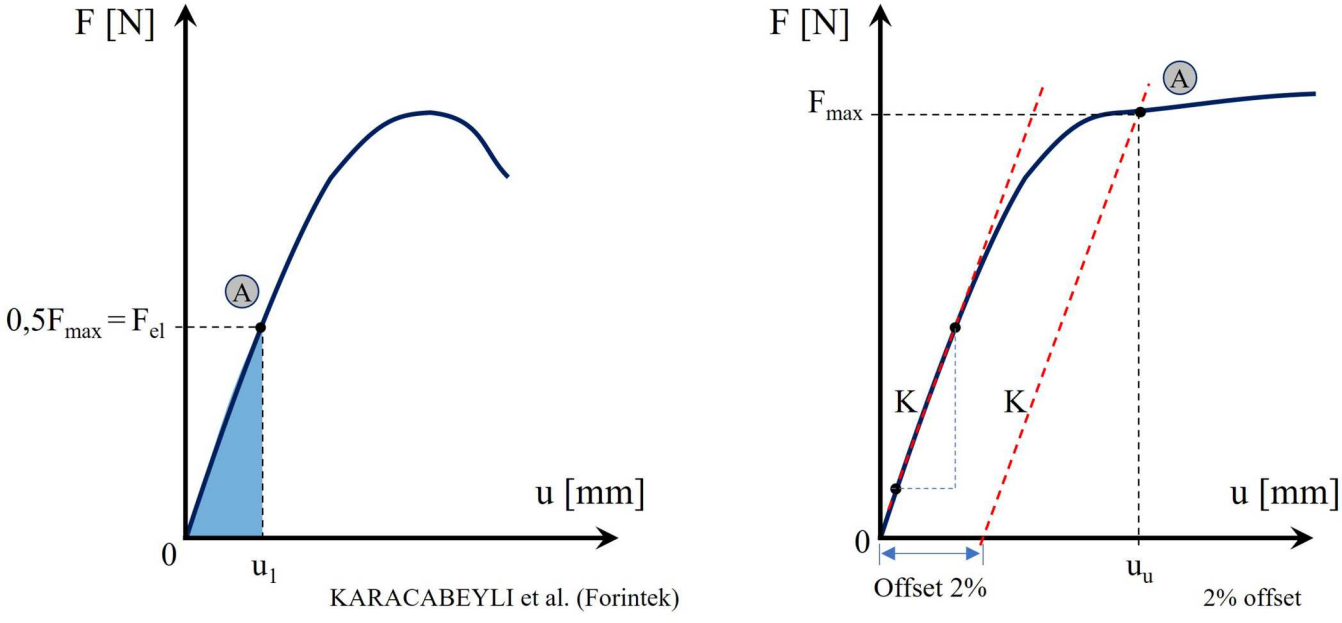

Figure 4. Left: Forintek method by Karacabeyli and Ceccotti to find yield deformation; Right: Offset method to find maximum force capacity.

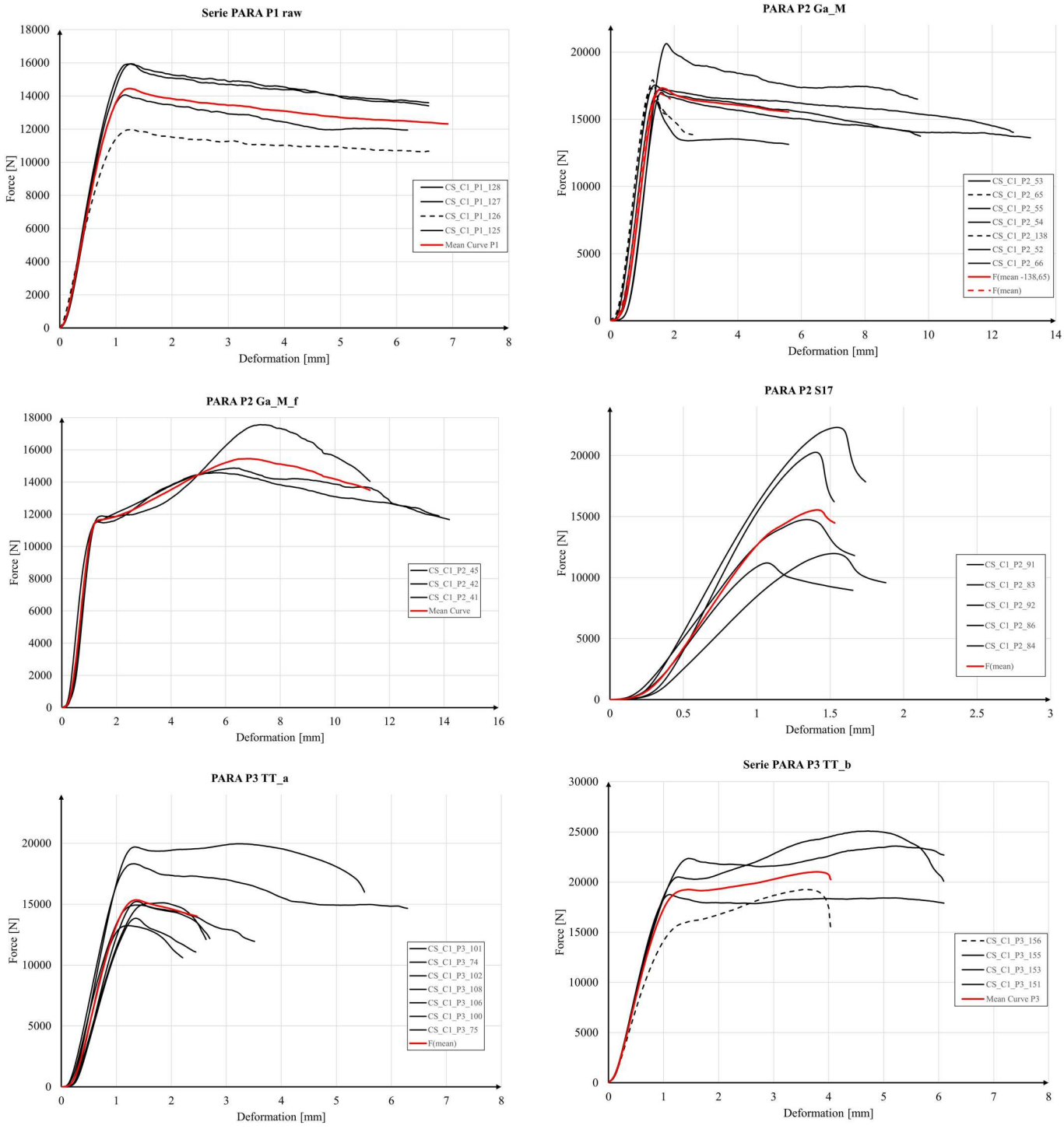

Figure 5. Compression test results of every specimen in PARA series: Up-left – raw wood; Up-right – gelatine stabilized (f-serie); Mid-left – gelatine stabilized; Mid-right – stabilizing resin stabilized; Down-left – TT stabilized (a-serie); Down-right – TT stabilized (b-serie).

parallel-to-grain compression, with results exhibiting significant noise (Figure 5, mid-right), potentially caused by variations in polymer infiltration. While the strength and stiffness were comparable to raw specimens, the ductility was considerably lower. The TT_a series (green curve) exhibited behaviour somewhat similar to the S17 series in terms of strength and stiffness but showed improved ductility, especially when individual specimens were considered (Figure 5, down-left). However, the TT_b series (dark green curve) outperformed all other PARA series, achieving a 33% increase in strength and a 21% increase in stiffness while maintaining relative ultimate ductility. Its balanced performance makes it the most favourable polymer-treated specimen within the PARA series.

In the SENK series, stabilization using different polymers led to consistent improvements in stiffness and strength across all specimens, as shown in Figure 6 (right). The Ga_M series (gold curve) displayed a 70% increase in strength and a 52% increase in stiffness. However, this came with a slight reduction in ductility, down to 90% of the raw wood

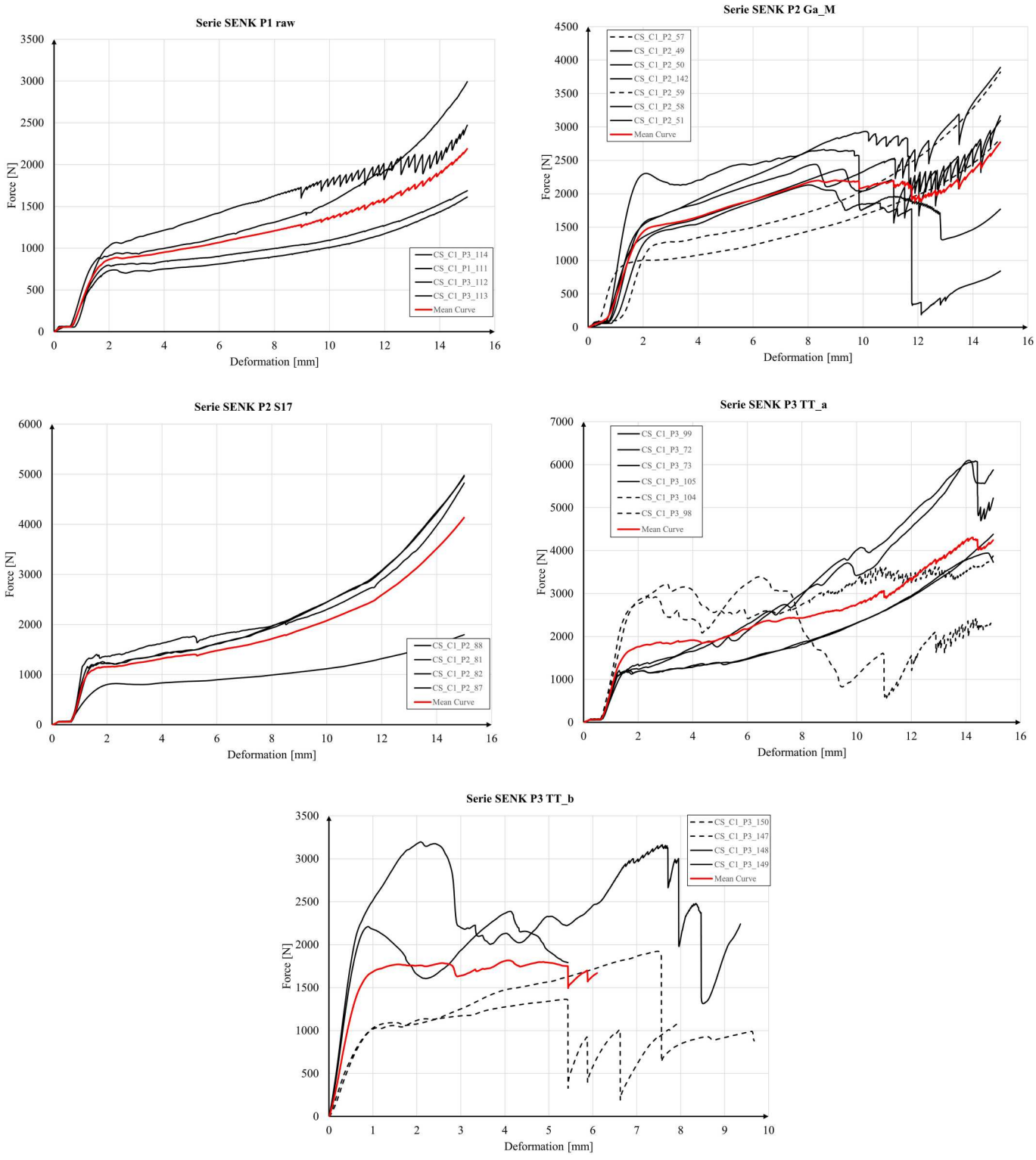

Figure 6. Compression test results of every specimen in SENK series: Up-left – raw wood; Up-right – gelatine stabilized; Mid-left – stabilizing resin stabilized; Mid-right – TT stabilized (a-serie); Down – TT stabilized (b-serie).

specimen. Furthermore, failure in this series became more chaotic after yielding, often accompanied by delamination. The S17 series (blue curve) showed the most similarity to the raw specimens, with strength increasing by 33% and stiffness by 80% while maintaining ductility at the same level as the untreated samples. TT_a and TT_b series exhibited significant strength improvements, with both having mean strength values approximately double that of the raw specimens (Figure 6, mid-right and down). TT_a series exhibited 21% greater stiffness but suffered from reduced ductility. TT_b, however, delivered exceptional results, achieving 2.8 times the stiffness and 1.5 times the ductility of the raw wood specimens. Both TT_a and TT_b series displayed unique behaviours during compaction, including timber grain wrinkling and unpredictable delamination occurring after 10% strain. These behaviours showed the need for

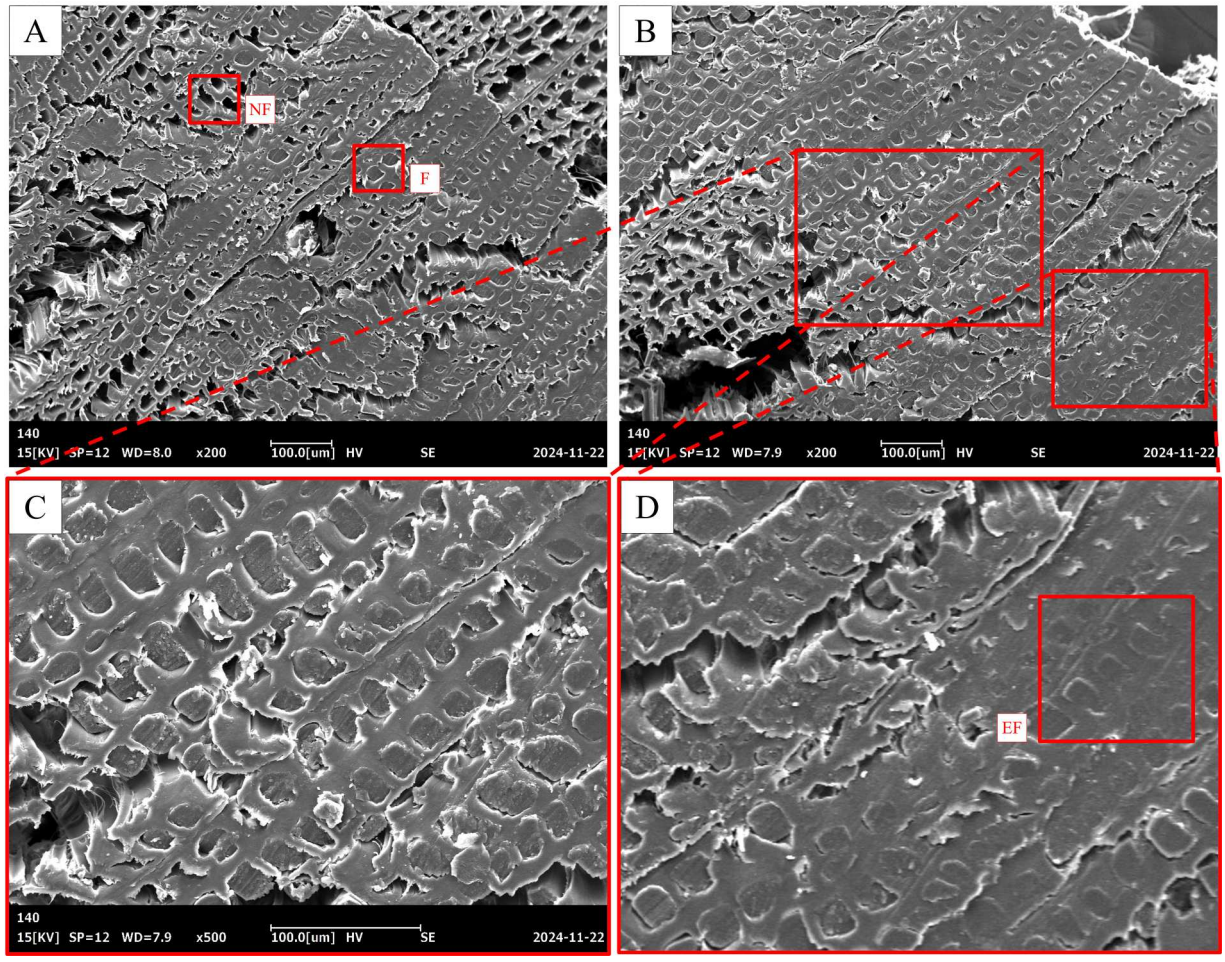

Figure 7. Images from the scanning electron microscopy (SEM) of the specimen CS_C1_P2_140 (Ga_M). The images (A) and (B) show different areas in the cross-section. (C) and (D) representing a close-up of image (B).

further study into their short- and long-term performance and failure characteristics, particularly as some series show the potential to enhance mechanical performance.

Results: SEM microscopic analysis and biodegradability determination

SEM microscopic analysis

The scanning electron microscopy (SEM) images show the successful infiltration of the wood with the gelatine-based solution (Figure 7). Filled voids (F) tend to be a darker shade of grey than the adjacent wood structure. The bedding has a strip-like structure in the direction of flow and is framed by a light, whitish ring of wood vessels. Unfilled cavities (NF), on the other hand, are black. Some larger structures are completely destroyed, these illustrate the irregularity of the wood or represent fractures caused by the previous separation of the wood slices from the specimen. Gelatine predominantly accumulates within the cell vessels, though some cell cavities were not reached. There are areas that are either completely permeated or completely empty. The incomplete filling could be attributed to the viscosity and penetration behaviour of gelatine, which may vary with temperature and moisture, causing uneven filling. Visually, in areas where gelatine was deposited, an irregular adhesion can be detected. Some cavity walls seem to be evenly filled (EF) and connected with the substance and create an almost uniform surface, which can only be distinguished by slightly lighter edges. While other cavity walls show an absence of adhesion, visible by a small gap between the substance and the wall. It is assumed that the solution was in the entire cavity at the time of infiltration, but that some of the water evaporated during the curing and drying process, and the cavity was therefore not completely filled. Furthermore, the wood's porosity and pore structure, as well as differences in gelatine concentration or preparation, could impact the substance's ability to infiltrate. According to Goldhahn *et al.* (2020), an increasing gelatine concentration may promote better adhesion to the cell interface. Following the path of the infiltrated solution, some cell walls were fractured, recognized by little cracks, likely due to the high vacuum pressure and the introduction of gelatine during treatment. Similar findings are described by Lemaire-Paul *et al.* (2023).

Biodegradability determination

After one week in soil, all specimens had an increase in weight, with the raw material exhibiting the highest increase at 78% and stabilizing resin the lowest at 34%. The strongest discolouration got to be recognized from the raw specimen, followed by the gelatine composite, indicating higher

Raw	Gelatine (Ga_M)	Turntex_a (TT_a)	Stabi17 (S17)
CS_C1_P1_115	CS_C1_P2_63	CS_C1_P3_97	CS_C1_P2_79
0 weeks (start)			
			
Weight: 4.6 g Start: **100 %**	Weight: 5.3 g Start: **100 %**	Weight: 6.1 g Start: **100 %**	Weight: 4.9 g Start: **100 %**
1 week			
			
Weight: 8.2 g Change: (**+78** %)	Weight: 8.6 g Change: (**+62** %)	Weight: 8.2 g Change: (**+34** %)	Weight: 7.5 g Change: (**+53** %)
3 weeks			
			
Weight: 7.8 g Change: (**+70 %** / -8 %)	Weight: 10.0 g Change: (**+88 %** / +16 %)	Weight: 8.1 g Change: (**+33 %** / -1 %)	Weight: 8.3 g Change: (**+69 %** / +16 %)
4 weeks			
			
Weight: 7.1 g Change: (**+54 %** / -16 %)	Weight: 9.8 g Change: (**+85 %** / -3 %)	Weight: 7.4 g Change: (**+21 %** / -12 %)	Weight: 7.5 g Change: (**+53 %** / -16 %)

Figure 8. Specimens differentiated by infiltration, staggered by weeks. The weight change compared to the original weight (in bold) and the change compared to the previous week are determined.

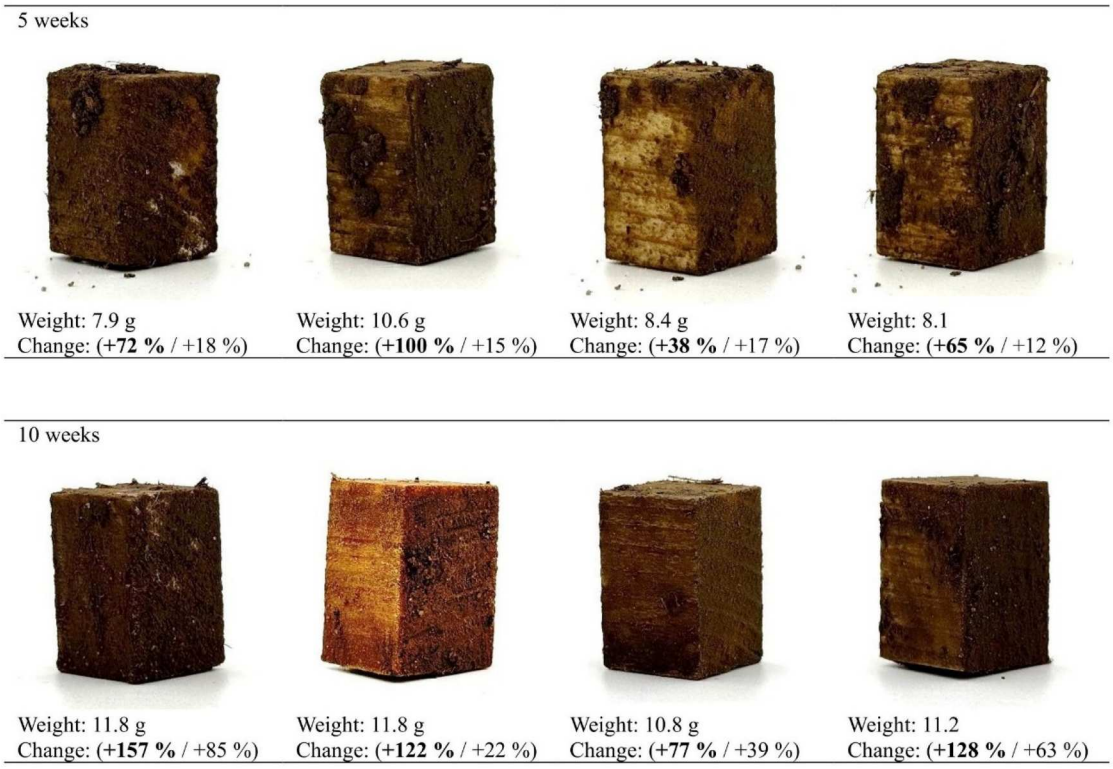

Figure 8 *Continued*

moisture uptake, consistent with the weight gain values (Figure 8). The difference between raw material and wood composites is attributed to the infiltration process, as the voids in the wood are blocked, preventing external influences from affecting the specimens. The specimens showed slight swelling. After three and four weeks, all specimens continued to show a weight increase compared to the weight at the beginning. Though, comparing the weight of week four with week three there is a clear decrease in weight, likely influenced by external fluctuations, particularly due to rain-periods. Discolouration intensified, with more soil adhering to the surface of the raw specimen, and fungal growth was observed on its upper half. After four weeks, swelling was clearly visible, especially at the base of the specimens. After five weeks, all specimens showed a weight increase, with the gelatine-treated specimen exceeding the raw specimen. Gelatine was suspected to attract water, though it is not believed to promote decomposition; similar findings were reported by Goldhahn *et al.* (2020). The discolouration continued to increase. After 10 weeks, all specimens showed a weight increase, with the raw specimen having the highest change at 157% and stabilizing resin the lowest at 77%. Discolouration intensified, with the gelatine-treated specimen showing an orange-like colour and the fibre direction becoming less visible in all specimens. All specimens were cleaned before analysing, still the reference and MMA specimens exhibited the most soil adhesion. Stabilizing resin showed the least swelling, while the other specimens showed swelling, deformation, and increased edge curves. Stabilizing resin demonstrated the highest resistance to biodegradation, followed by gelatine. However, it is important to note that while weight gain was observed after 10 weeks and infiltrated specimens showed less weight gain, the results cannot conclusively determine biodegradability. A 10-week period is insufficient, and long-term trials with additional specimens from the same composite are needed for definitive conclusions. Cutting open the test specimens after 10 weeks revealed only slight differences in colour (Figure 9). The infiltrated specimens with MMA showed a brownish discolouration along the growth rings. In addition, the cutting edge is smooth compared to the other test specimens. The wood composites with gelatine and stabilizing resin in particular have an uneven, pitted surface.

Results: relative water absorption

A series of tests was performed on six specimens of raw timber to assess their weight and moisture behaviour under varying conditions. The raw series in Table 6 shows moderate variability between specimens, what is expected noise in timber material behaviour. This variability can be seen after soaking specimens in water with different increases in weight and moisture caused by non-uniformity of wood.

In case of Gelatine (Ga_M) treatment significantly increased initial weight and moisture (very high effect sizes). After soaking, treated wood was heavier ($p = 0.0013$, $d = 2.81$), but absorbed a similar percentage of water. Visible changes, such as gelatine swelling around the edges of the specimens, can be observed. Moisture after drying stayed higher (15.7% vs. 12%, $p < 0.001$), showing gelatine causes lasting water retention. S17 specimens showed moderately increased initial and dry weight compared to RAW, but differences weren't statistically significant ($p = 0.10$–0.93, $d \approx 1.0$–1.3), suggesting some effect but not consistent enough across

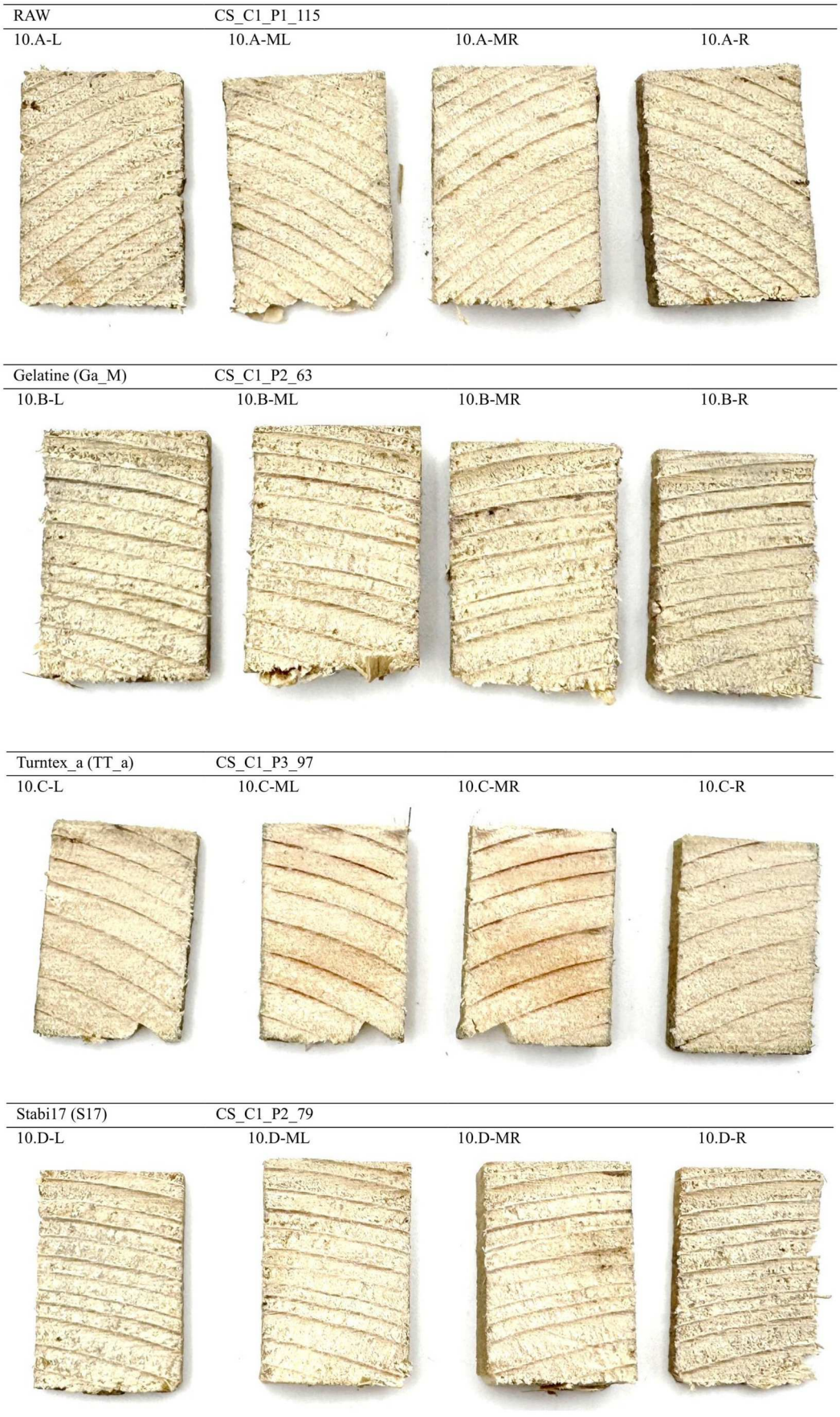

Figure 9. Specimens differentiated by infiltration, after 10 weeks in soil, cut into 4 parts.

Table 6. Average results of water absorption test per substance treatment with statistical validation.

			RAW			Ga_M				S17				TT			
			x̄			x̄				x̄				x̄			
	SERIES		ME	S		ME	S	*p*	Cd	ME	S	*p*	Cd	ME	S	*p*	Cd
Weight	initial	[g]	**4.2**			**5.9**					**5.1**				**7.3**		
			±001	0.85		±000	0.46	0.0026	2.53	±001	1.00	0.1018	0.96	±001	1.21	0.0006	1.92
	saturated after 24h	[g]	**6.1**			**8.2**					**6.5**				**8.5**		
			±001	0.93		±000	0.52	0.0013	2.81	±001	0.92	0.4519	2.28	±001	1.11	0.0027	1.91
	increase	[%]	**68%**			**71%**					**78%**				**85%**		
			±008%	8.97%		±003%	3.07%	0.4151	0.50	±004%	4.17%	0.0412	1.82	±004%	4.24%	0.0036	1.72
	dry after water absorption	[g]	**5.2**			**6.3**					**5.2**				**7.0**		
			±001	0.87		±000	0.51	0.0316	1.50	±001	1.00	0.9282	1.28	±001	1.32	0.0236	1.47
Moisture	initial	[%]	**8%**			**12%**					**8%**				**10%**		
			±000%	0.44%		±000%	0.41%	0.0000	8.05	±000%	0.53%	0.5690	6.83	±001%	1.06%	0.0106	1.76
	saturated after 24h	[%]	**25%**			**29%**					**22%**				**22%**		
			±006%	5.91%		±006%	6.81%	0.3169	0.61	±005%	5.23%	0.4577	1.11	±003%	3.01%	0.3322	0.10
	increase	[%]	**17%**			**18%**					**14%**				**12%**		
			±006%	5.89%		±006%	6.67%	0.8680	0.10	±005%	5.55%	0.4405	0.57	±003%	3.14%	0.1541	0.42
	dry after water absorption	[%]	**13%**			**16%**					**13%**				**13%**		
			±001%	0.75%		±001%	1.03%	0.0002	3.37	±001%	0.63%	0.2720	3.11	±001%	1.05%	1.0000	0.58

Note: x̄ – mean value; ME – margin of error indicating confidence level; S – standard deviation; *p*-value – acquired with *T*-Test (unequal variance); Cohen´s *d* – shows the size of effect.

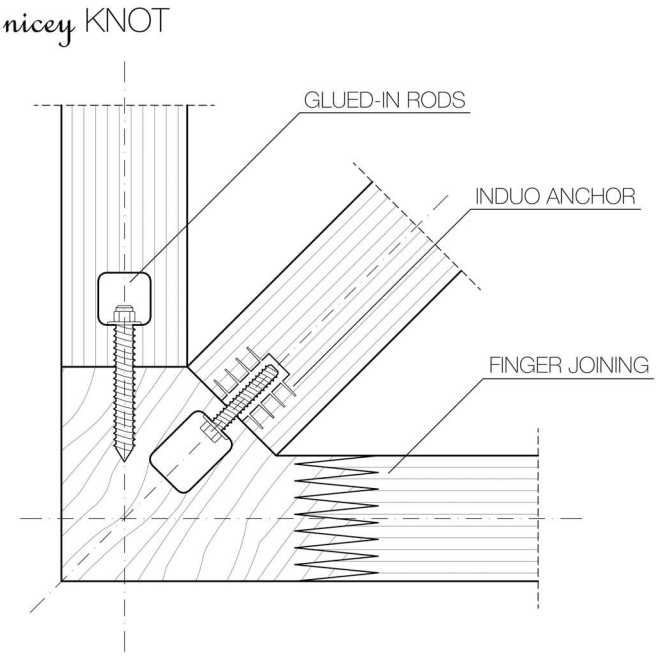

Figure 10. Application as a knot connection. "niceyKnot" made from stabilized spruce wood. Can be modified depending on the connections, e.g. glued-in rods, induo anchor, finger joining.

samples. Water absorption increased significantly ($p = 0.041$, $d = 1.82$), meaning S17 retained more water than RAW. Post-soaking weight rose (6.53 g vs. 6.12 g), but the difference wasn't significant ($p = 0.45$). S17 slightly altered absorption behaviour, with high variability and mixed statistical support. In comparison TT_a specimens showed a big increase in weight across all stages – initial, soaked, and dried – with very strong effects ($p < 0.003$, Cohen's $d \approx 1.9$). Water absorption was also higher than RAW ($p = 0.0036$, $d = 1.72$), confirming TT_a treatment increased water uptake. Post-drying weight was significantly higher as well ($p = 0.0236$, $d = 1.47$), indicating lasting material change. Overall, TT_a made the wood heavier, more absorbent, and structurally altered compared to RAW.

The results suggest that the superior water resistance observed in synthetic polymer treatments is likely attributable to the hydrophobic nature of the methyl methacrylate-based resin, which forms a more continuous, moisture-impermeable network within the wood structure. This polymer likely reduces capillary flow through the cell wall microstructure, explaining the reduced water uptake. In contrast, gelatine-based polymers are hydrophilic in nature and prone to swelling or partial dissolution in moisture-rich environments. This likely contributed to their relatively poor water resistance. According to the research of Naïssi *et al*. (2024), a higher gelatine concentration or the addition of additives can reduce the water absorption capacity. However, this hydrophilic behaviour is also a key reason for their superior biodegradability.

Possible practical structural application

The modified wood composite has an increased hardness and improved dimensional stability, these properties offer suitable application, especially for high-stress areas.

Truss joints and knot connections: "niceyKNOT"

The primary application areas are truss joints and knot connections. In truss joints, high stress concentrations arise due to intersecting members and fasteners. These regions are particularly susceptible to splitting, deformation, or creep, especially under cyclic or dynamic loading conditions. Stabilized wood exhibits increased density and load-bearing capacity, thereby reducing the risk of joint failure. Its dimensional stability prevents swelling, shrinking, or warping under fluctuating environmental conditions, ensuring long-term joint integrity. Furthermore, its resistance to splitting makes it particularly suitable for locations with pre-drilled holes for bolts, screws, or dowels. In trusses, forces are transmitted through joints where compressive and tensile forces converge. Stabilized wood inserts can act as buffers or reinforcements around boltholes, mitigating stress concentrations and promoting more uniform load distribution. As illustrated in Figure 10, such inserts could be implemented at the knots of diagonal and vertical members, particularly in the bottom chords where tensile forces predominate. Furthermore, a uniform density contributes to an even load distribution.

This approach is also applicable to wooden bridge trusses or large timber roof trusses in humid environments, where conventional joints are prone to degradation. Additionally, historic reconstructions, such as timber-framed churches or barns, could benefit from stabilized wood to enhance long-term structural stability while preserving the aesthetic authenticity of the original construction.

Reinforcement around fasteners

Stabilized wood's enhanced density and stiffness make it ideal for localized reinforcement in high-load zones like beam-column connections. It prevents splitting or deformation around fasteners, improving durability and reducing the risk of loosening due to creep or deformation. By evenly distributing loads, it reduces localized stress, particularly in connections with oversized holes or frequent assembly and disassembly. The resin-filled structure minimizes micro-movements, ensuring long-term fastener stability. This makes stabilized wood especially valuable in high-wear applications like observation towers or pedestrian bridges exposed to weathering and repeated use.

Structural retrofits and repairs

Stabilized wood is ideal for retrofitting or repairing damaged structural elements, such as cracked beams, split columns, or degraded joints. By infiltrating weak points or cracks with polymers, it restores load-bearing capacity and creates a reliable load path to transfer forces around damaged areas. This targeted approach not only reinforces the structure but also extends its lifespan through precise, localized stabilization.

Hybrid connections in wood-metal structures

Stabilized wood is highly effective in hybrid connections where wood meets metal, such as steel gusset plates or brackets. Its dimensional stability prevents loosening, while resistance to moisture and decay ensures durability in outdoor or marine environments. By resisting localized crushing under metal fasteners, stabilized wood maintains consistent load transfer and reduces shear stress concentrations. In hybrid wood-metal trusses, it serves as an intermediary, securing bolts and rivets in place. Additionally, its compatibility with adhesives enhances load distribution in glued hybrid systems. Applications include retrofitting historical timber-steel railway bridges to extend their lifespan and incorporating stabilized wood in modern high-end structures like designer pavilions or eco-friendly hybrid skyscrapers for improved durability and sustainability.

Compression members in decorative structures

Stabilized wood is ideal for compression members in lightweight or decorative structures like pergolas, pavilions, or interior trusses. Its higher density supports greater compressive loads and reduces buckling risks due to its increased modulus of elasticity. In structures like gazebos, stabilized wood columns distribute roof loads uniformly along the axis, minimizing deformation. Its homogeneity ensures consistent performance, even under eccentric loads, where conventional wood might become unstable. Additionally, its resistance to environmental degradation preserves the structural integrity of decorative elements over time.

Conclusion

The results of this study demonstrate that vacuum-assisted polymer infiltration significantly enhances the mechanical performance and environmental resistance of wood, offering valuable improvements for structural applications. The mechanical reinforcement strongly correlates with the type of polymer used, infiltration depth, and wood species. Synthetic polymer-treated specimens, particularly those infiltrated with methyl methacrylate (MMA, TT_b series), showed the most pronounced improvements in compressive strength and stiffness, owing to their low viscosity and high infiltration efficiency (Pw = 63%). Gelatine-based biopolymers (Ga_M series), while more sustainable, demonstrated limited penetration and only moderate gains in mechanical performance, primarily due to their higher viscosity and partial distribution confined to cell lumens, as confirmed by SEM analysis. Furthermore, environmental testing revealed notable differences in moisture behaviour and biodegradability. MMA and stabilizing resin-treated specimens showed reduced water uptake and better moisture stability, in contrast to the gelatine-treated samples, which retained higher moisture content and showed pronounced swelling. However, the bio-based specimens also exhibited superior biodegradability, underlining the trade-off between environmental durability and ecological sustainability. These results indicate that synthetic polymers form more effective hydrophobic networks within the wood matrix, while biobased polymers prioritize environmental compatibility.

From a practical standpoint, the enhanced performance of infiltrated wood is particularly relevant for high-stress structural components such as truss joints, knot zones, or areas exposed

to cyclic loading and harsh climatic conditions. The ability to tailor polymer systems for specific performance profiles could open new possibilities for durable, lightweight, and sustainable timber components in construction.

In conclusion, this study demonstrates that vacuum infiltration significantly improves wood mechanical properties, with synthetic polymers providing superior reinforcement and water resistance, while biobased polymers offer an eco-friendly alternative. Future research should focus on optimizing polymer formulations for durability, including long-term durability testing exposed to different environmental conditions such as UV radiation or microbial attack, conducting life cycle assessments and evaluating large-scale implementation feasibility.

Acknowledgements

The authors would like to express their sincere gratitude to the Institute of Technical and Macromolecular Chemistry (ITMC), Chair of Heterogeneous Catalysis and Technical Chemistry, RWTH Aachen University, Aachen, Germany, for the use of their SEM facilities and their valuable assistance. The company "Drechseln und mehr" for the utilization of the infiltration fluid, D&M Stabi 17 S Vakuumharz. The company TurnTex, LLC for the utilization of the infiltration fluid, Cactus Juice Stabilizing Resin.

Disclosure statement

No potential conflict of interest was reported by the author(s).

ORCID

Maria Naissi http://orcid.org/0009-0006-9411-6793

References

Augustina, S., *et al*., 2024. Treatability and dimensional stability of three hardwood species using different types of water-soluble impregnating agent. *European Journal of Wood and Wood Products*, 82, 1421–1433. doi:10.1007/s00107-024-02096-w.

Behr, G., 2020. *The influence of melamine treatment in combination with thermal modification on the properties and performance of native hardwoods*. Doctoral thesis.

Bicke, S., 2019. *Dimensionsstabile und pilzresistente Furnierwerkstoffe durch Zellwandmodifizierung mit niedermolekularem Phenol-Formaldehyd*. Doctoral thesis.

Boonstra, M., 2016. Dimensional stabilization of wood and wood composites. *In*: N. Belgacem and A. Pizzi, eds. *Lignocellulosic fibers and wood handbook*. Hoboken, NJ: John Wiley & Sons, 629–655.

DIN 52183: 1977-11, 1977. *Testing of wood; determination of moisture content*.

DIN 52185:1976-09, 1976. *Testing of wood; compression test parallel to grain*.

DIN 52192:1979-05, 1979. *Prüfung von Holz; Druckversuch quer zur Faserrichtung*.

DIN CEN/TS 15534-2:2007, 2007. *Holz-Polymer-Werkstoffe (WPC)—Teil 2: Beschreibung von WPC-Werkstoffen*.

DIN EN 15534-1:2018-02, 2018. *Verbundwerkstoffe aus cellulosehaltigen Materialien und Thermoplasten—Teil 1: Prüfverfahren zur Beschreibung von Compounds und Erzeugnissen*.

DIN EN 26891:1991-07, 1991. *Holzbauwerke—Verbindungen mit Mechanischen Verbindungsmitteln—Allgemeine Grundsätze für die Ermittlung der Tragfähigkeit und des Verformungsverhaltens*.

DIN EN 408:2012-10, 2012. *Timber structures—structural timber and glued laminated timber—determination of some physical and mechanical properties*.

Dorr, D., *et al*., 2015. Bond strength of biodegradable gelatin-based wood adhesives. *Journal of Renewable Materials*, 3, 195–204. doi:10.7569/JRM.2015.634108.

Egner, S., and Dietsch, P., 2024. Experimental study to determine the development of axial stiffness of wood screws with increasing load cycles. *Buildings*, 14 (4), 1109. doi:10.3390/buildings14041109.

EN 12512—ISO/DIS 16670: 2001, 2001. *Timber structures. Test methods. Cyclic testing of joints made with mechanical fasteners*.

Goldhahn, C., *et al*., 2020. Wood–gelatin bio-composite membranes with tunable flux. *ACS Sustainable Chemistry & Engineering*, 8 (18), 7205–7213. doi:10.1021/acssuschemeng.0c01856.

Hartig, J.U., *et al*., 2023. Impregnation of wood with a paraffinic phase change material for increasing heat capacity. *Wood Material Science & Engineering*, 18, 19–28. doi:10.1080/17480272.2022.2133630.

Hunt, C., and Dunky, M., 2023. Analysis of future prospects and opportunities for wood adhesives: a review. *Forest Products Journal*, 72, 14–22. doi:10.13073/FPJ-D-23-00011.

Karacabeyli, E., and Ceccotti, A., 1996. *Quasi-static reversed-cyclic testing of nailed joints*. Available from: https://www.cabidigitallibrary.org/doi/full/10.555519970605212.

Kolbe, J., *et al*., 2023. Glued-in hardwood rods using bio-sourced adhesives – part I: investigations under laboratory conditions. *In*: *World Conference on Timber Engineering (WCTE 2023)*, 804–811.

Lemaire-Paul, M., *et al*., 2023. The impact of vacuum pressure on the effectiveness of SiO2 impregnation of spruce wood. *Wood Science and Technology*, 57 (1), 147–171. doi:10.1007/s00226-022-01448-0.

Matejak, M., and Kozakiewicz, P., 2011. Die Reindichte der Zellwandsubstanz. *Annals of Warsaw University of Life Sciences – SGGW. Forestry and Wood Technology*, 75, 85–90. Available from: http://agro.icm.edu.pl/agro/element/bwmeta1.element.agro-fe4ce8b2-61d4-4774-8895-f9bc6b12fab1.

Naïssi, M., *et al*., 2024. *Shifting towards eco-responsible construction: Bio-based and bio-degradable polymers as substitutes for synthetic membranes*.

Neyses, B., *et al*., 2017. Pre-treatment with sodium silicate, sodium hydroxide, ionic liquids or methacrylate resin to reduce the set-recovery and increase the hardness of surface-densified Scots pine. *iForest – Biogeosciences and Forestry*, 10, 857–864. doi:10.3832/ifor2385-010.

Niemz, P., and Sonderegger, W.U., 2021. *Holzphysik: Eigenschaften, Prüfung und Kennwerte*, 2., aktualisierte Auflage. München: Hanser.

Patachia, S., and Croitoru, C., 2016. Biopolymers for wood preservation. *In:* F. Pacheco-Torgal, V. Ivanov, N. Karak, and H. J. Kidlington, eds. Kidlington: Elsevier Ltd, 305–332.

Rui, H., *et al*., 2019. Spalting colorants as dyes for wood stabilizers. *Journal of Coatings Technology and Research*, 16 (3), 905–911. doi:10.1007/s11998-019-00203-8.

Sandberg, D., *et al*., 2021. *Wood modification technologies: principles, sustainability, and the need for innovation*. 1st ed. Boca Raton, FL: CRC Press/Taylor & Francis Group.

Schneider, M., 1994. Wood polymer composites. *Wood and Fiber Science*, 26, 142–151.

SIA 265: 2003, 2003. *Swiss code for timber structures*. Zürich: Swiss Society of Engineers and Architects.

Smith, I., and Foliente, G., 2002. Load and resistance factor design of timber joints: international practice and future direction. *Journal of Structural Engineering*, 128 (1), 48–59. doi:10.1061/(ASCE)0733-9445(2002)128:1(48).

Stefanowski, B.K., Spear, M.J., and Pitman, A., 2018. *Review of the use of PF and related resins for modification of solid wood*.

Tondi, G., *et al*., 2012. Tannin-boron preservatives for wood buildings: mechanical and fire properties. *European Journal of Wood and Wood Products*, 70 (5), 689–696. doi:10.1007/s00107-012-0603-1.

Wehsener, J., Bremer, M., and Haller, P., 2023. *Mechanical properties tests of delignified and densified wood*, p. 704.